SUK, M.-O., JO, S.-K., SEO, C.-W., KIM, S.-H., KIM, J.-S., SHIM, S.-C., and KIM, J.-T. The effect of carbon in slag on steel reoxidation by CaO-SiO_2-Al_2O_3-MgO-MnO-Fe_tO slags. *VII International Conference on Molten Slags Fluxes and Salts,* The South African Institute of Mining and Metallurgy, 2004.

The effect of carbon in slag on steel reoxidation by CaO-SiO_2-Al_2O_3-MgO-MnO-Fe_tO slags

M.-O. SUK*, S.-K. JO*, C.-W. SEO*, S.-H. KIM*, J.-S. KIM†, S.-C. SHIM‡, and J.T. KIM§

**Pohang University of Science and Technology, Materials Science and Engineering, Pohang, Kyungbuk, Korea*

†Gwangyang Works, Kumho-dong, Gwangyang, Chollanam-do, Korea

‡Technical Research Laboratories, Koedong-dong, Nam-gu, Pohang, Kyungbuk, Korea

§R&D Center Production Division, Doosan Heavy Industries & Construction Co., Changwon, Gyongnam, Korea

An equilibrium study was carried out at 1873 K to ascertain the effect of carbon in CaO-SiO2-Al_2O_3-MgO-MnO-Fe_tO slag systems on their Fe_tO and MnO activity coefficients, representing the slag's thermodynamic potential for steel reoxidation. Both γ_{Fe_tO} and γ_{MnO} showed not only a sharp increment, but also a simultaneous slow decrement by increasing carbon content in slag, suggesting opposite roles of the carbon according to its stable forms. XPS (X-ray photoelectron spectroscopy) was introduced to clarify the stable forms of carbon in slag. XPS results prove that carbon dissolves in slag as carbonate, and carbide ions under oxidizing and reducing atmospheres, respectively. It was concluded that carbonate ions increase γ_{Fe_tO} and γ_{MnO}, and that carbide decreases them. This paper suggests an application method of the present results to actual ladle refining processes, in order to enhance steel cleanliness without decreasing (Fe_tO + MnO) content in slag.

Keywords: carbon, slag, activity coefficient, Fe_tO, MnO, carbonate, carbide, XPS, reoxidation, cleanliness

Introduction

There has been an increasing demand for ultra-clean high-grade steels with minimum amounts of inclusions. The reduction of oxide inclusions is performed by flotation into the slag phase and by prevention of Al reoxidation in steel during ladle refining operations. Steel reoxidation by reducible oxides in slag, such as Fe_tO and MnO, induces the formation of fine inclusions, which are not easily floatable during the refining stage. Therefore, for the production of ultra-clean steels, it is important to decrease the activity of the reducible oxides causing the steel reoxidation.

In ladle refining processes, (Fe_tO + MnO) content in slag should be lowered less than 1 wt% for the effective desulphurization and the suppression of the steel reoxidation. This brings about an increase in production cost and processing time because of the excessive injection of raw materials. Decreasing the activity coefficients of Fe_tO and MnO is an alternative solution for controlling the activities of the reducible oxides while maintaining high (Fe_tO + MnO) content.

The slag phase will contain a certain degree of carbon. Previous research confirms that carbon in Cr_2O_3 containing slag reduces the activity coefficients of Fe_tO and MnO[1]. It is necessary to investigate in more detail the activity behaviours of reducible oxides in carbon containing slags to minimize steel reoxidation. However, studies on carbon containing slags have focused mainly on solubility and stable forms of carbon in slag[2–6]. To date there have been no reports on the effect of carbon in slag on the activities of Fe_tO and MnO. So, in this work, the thermodynamic equilibria between CaO-SiO_2-Al_2O_3-MgO-MnO-Fe_tO slag systems and liquid iron were been carried out in MgO crucible at 1873 K varying the carbon content in slag. The activity coefficients of Fe_tO and MnO, which affect the steel cleanliness, will be discussed, stressing the effect of carbon in slag.

To clarify the stable form of carbon in slag, XPS (X-ray photoelectron spectroscopy) was introduced. Park *et al.* showed the possibility of XPS application for the analysis of carbon in iron ore[7]. From the XPS results, we will ascertain the dominant parameters affecting the activity coefficients of Fe_tO and MnO. Finally, this paper will suggest an application method of the present results to actual ladle refining processes in order to enhance the steel cleanliness under the condition of high (Fe_tO + MnO) content.

Experimental

The equilibrium study between slag and metal was carried out at 1873 K under an Ar atmosphere in a $LaCrO_3$ resistant furnace equipped with a fused alumina tube of 50 mm diameter and a hot zone length of 5 mm. The tube was sealed at both ends with water-cooled brass lids. Argon was purified through, in sequential order, H_2SO_4, P_2O_5, $Mg(ClO_4)_2$, a bed of Ti-granules at 620°C, $Mg(ClO_4)_2$ and was then released into a reaction tube. The schematic diagram of the experiment apparatus is shown elsewhere in detail[8].

The master slags were prepared by pre-melting the mixtures of reagent grade $CaCO_3$, SiO_2, Al2O_3 and MgO in a graphite crucible, then crushed to a size below 60 mesh and baked at 1200°C for 24 hours for decarburization. The initial carbon in metal was fixed at 1 wt%. The essential

factor, carbon content in slag (the sum of carbide and carbonate contents), is strongly dependent on the oxygen potential of a contacting phase (gas or metal) as shown in Figure 1[9]. In this work, oxygen potential was controlled by varying the degree of steel deoxidation, i.e. the amount of aluminum and silicon. 30g of metal composed of high-purity electrolytic iron ([%O]=0.0035, [%Al]=0.0003, [%C]=0.001, [%Si]<0.001), Fe-10 pct Al, Fe-10 pct Si, Fe-20 pct Mn, Fe- 6.1 pct C and FeS, and 7g of CaO-SiO_2-Al_2O_3-MgO master slag were melted using an MgO crucible. The melts were stirred over a period of 2 hours by an Al_2O_3 rod for 30 seconds at 30-minute intervals to facilitate the equilibrium between slag and metal. To eliminate oxide inclusion by flotation, melts were not stirred for 3 hours before quenching. The time for equilibration was preliminary determined. After equilibrating the melts for 5 hours, the crucible was pulled out of the furnace and rapidly quenched in cold water.

The silicon, aluminum, manganese, calcium and magnesium in metal samples were analysed by inductively coupled plasma emission spectrometry and oxygen by inert-gas fusion infrared absorptiometry. The total carbon and sulphur content in the metal and slag were analysed by oxygen-gas fusion infrared absorptiometry. The equilibrium slag compositions were determined using X-ray fluorescence spectroscopy.

XPS (X-ray photoelectron spectroscopy) was used to clarify the stable forms of carbon in slag such as carbonate, carbide ions and graphite. Because of the XPS characteristic, it is very important for surfaces to be flat and smooth in order to get uniform reflection intensity and to remove the other error sources. Therefore, molten slag was quickly poured on a cold Cu plate on cold water and was then pressed by a Cu bar. After setting the sample in the XPS equipment, the surface of the sample was etched by an Ar gas stream to clean up the surface before the main XPS analysis step. A wide scan for all the elements in the slag was tried to examine the existing atoms and the possibility of carbon detection. A typical wide scan result is shown in Figure 2.

Carbon species were found in the 270~300eV range, which was used for all XPS analyses in this work. Three peaks regarding carbon species were observed for a slag sample as shown in Figure 3. A literature survey indicates that carbon exists in slag as forms of carbonate and carbide ions[2,4,10]. The remaining peak was presumed to represent graphite. To confirm the three peaks as carbonate ions, graphite, and carbide ions, a reference sample was analysed by XPS as shown in Figure 4. The sample was a physically mixed powder of calcium carbonate, graphite, and calcium carbide. The two peaks for carbonate ions and graphite agree with reported peaks in the previous works, Christie *et al*. (Carbonate-289.6 eV)[11] and Palchan *et al*. (Graphite-284 eV)[12], and the remaining peak is thought to be carbide ions by the above mentioned literature survey.

The three peaks in Figure 3 coincide with the reference peaks in figure 4 and, therefore, are inferred to be carbonate ions, graphite and carbide ions. The well-known and comparatively accurate Al peak (74.3 eV)[13] was used for the compensation of the charging effect of the carbon peak (a peak shift by vibration of atomic binding during etching). For a quantitative analysis of each peak, the curves were fitted by Gaussian curve fitting (the mathematical calculation method that averages the fluctuating curve and sums the area) and the amount of each species was obtained by dividing the total carbon content with each peak area fraction.

We found that the carbon in the same slag sample showed different analysis values according to the sample preparation form, as shown in Figure 5. The carbon

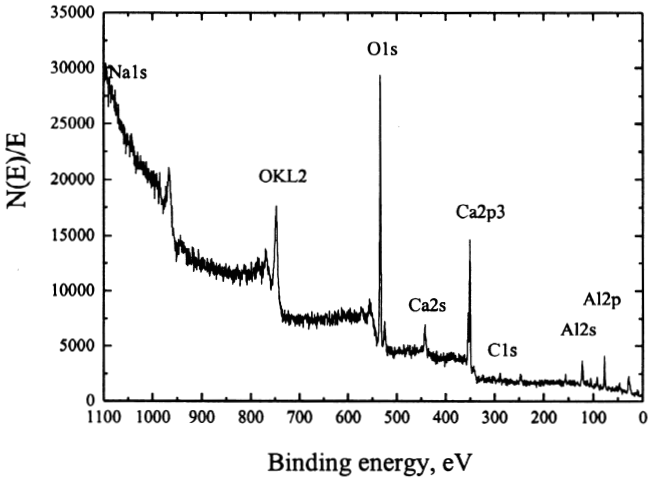

Figure 2. Wide scan result of XPS for all elements

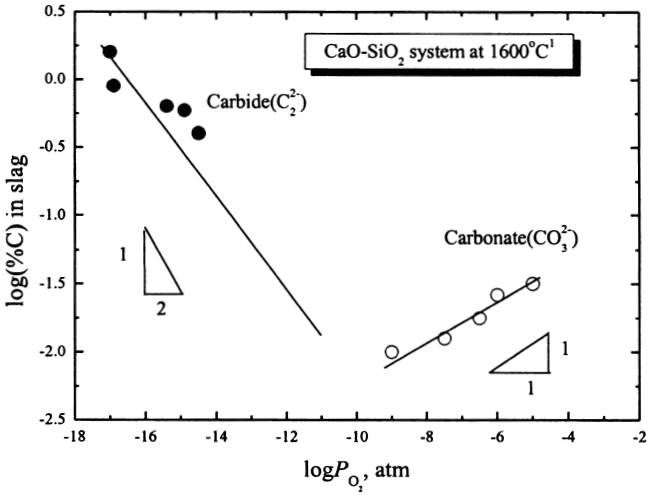

Figure 1. Carbon contents in CaO-SiO_2 slag systems at various oxygen partial pressures[1]

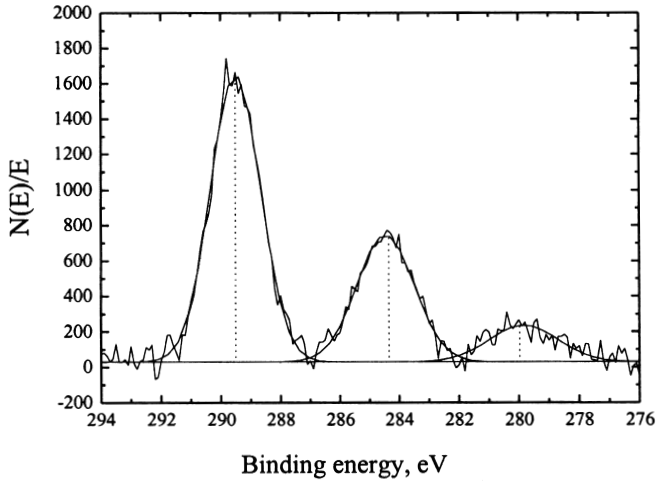

Figure 3. Carbon peaks analysed by XPS

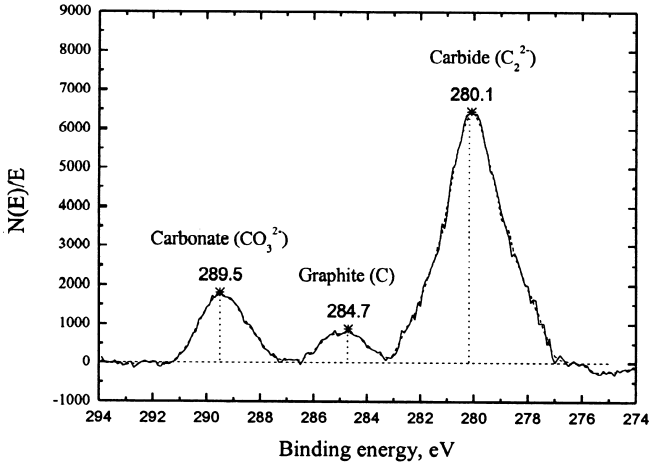

Figure 4. Reference peaks of carbide, graphite and carbonate (present work)

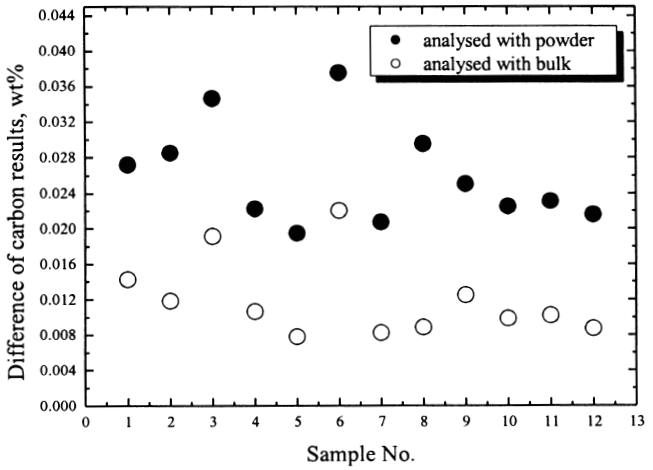

Figure 5. Difference in analysed carbon content between powder and bulk

contents analysed as a form of bulk display comparatively lower values than those as a form of powder. The sulphur contents in slag, which were simultaneously analysed with the carbon, showed no difference between powder and bulk forms. In order to exclude the possibility of incomplete melting of the bulk sample, the sample was re-melted, but no more carbon was detected. The higher carbon content in the powder sample may have been caused by dust materials in air during powdering slag samples. Besides, the XPS results prove the contamination phenomena of the samples. The graphite peak diminished continuously after up to 4 minutes of etching and thereafter remained constant as shown in Figure 6. There was no change in the peaks of carbonate and carbide ions. This means that the samples are contaminated as a form of graphite. Therefore, the etching time was chosen as 6 minutes to allow for adequate surface cleaning. In this paper, the carbon content in slag represents value analysed as a form of bulk.

Results and discussion

The equilibrium chemical compositions of metal and slag samples employed in this work are listed in Table I. The molar ratio of $(X_{CaO} + X_{MgO})/(X_{SiO_2} + X_{Al_2O_3})$ is used as a basicity in this context.

The activity coefficient of Fe_tO can be calculated using the equilibrium constant of the following reaction:

$$Fe(l) + \underline{O} = Fe_tO(l) \qquad [1]$$

$$\Delta G_1^0 = -116100 + 48.79T \text{ in J/mol}^{14}$$

$$K_1 = a_{Fe_tO} / a_O = \gamma_{Fe_tO} X_{Fe_tO} / f_O[\%O] \qquad [2]$$

where the activity of total iron oxide in slag is referred to with respect to a pure liquid standard state and the activity of oxygen in metal is determined relative to a 1% standard state (referring to mass contents). The γ_{Fe_tO} values can be obtained from Equation [2] by using the experimental results in Table I as well as the respective interaction parameters in Table II[15,16].

Figure 7 shows the effect of carbon in slag on its Fe_tO activity coefficient. The γ_{Fe_tO} value shows both increasing and decreasing tendencies with increasing carbon content. This means that carbon in slag works in two different ways on γ_{Fe_tO}. Fe_tO content does not affect its activity coefficient up to X_{Fe_tO}=~0.014, as shown in Figure 8. Ohta *et al*. also report the constancy of γ_{Fe_tO} up to X_{Fe_tO}=~0.03 in the CaO-SiO_2-Al_2O_3 slag system[17]. It is thus considered that γ_{Fe_tO} is not affected by Fe_tO content within the Henrian range of Fe_tO in slag. Therefore, the basicity and carbon in slag only influence γ_{Fe_tO}.

The manganese deoxidation equilibrium can be expressed as follows:

$$\underline{Mn} + \underline{O} = MnO\ (s) \qquad [3]$$

$$\Delta G_3^0 = -288100 + 128.3T \text{ in J/mol}^{18}$$

$$K_3 = a_{MnO} / a_{Mn} a_O = \gamma_{MnO} \qquad [4]$$

$$X_{MnO} / f_{Mn}[\%Mn] f_O[\%O]$$

where MnO activity is referred to with respect to solid standard state and oxygen activity in metal is determined relative to a 1% standard state (referring to mass contents). The γ_{MnO} values can be also obtained, as can those of γ_{Fe_tO}.

Figure 9 shows the behaviour of γ_{MneO} according to the carbon content in slag. Similarly to the case of γ_{Fe_tO}, the value of γ_{MnO} diverges in two ways by increasing carbon content. MnO content does not affect its activity coefficient up to X_{MnO}=~0.008 as shown in Figure 10 (obtained in the present work) and is generally considered to show a wider Henrian range (up to a molar mass fraction of ~0.1 in the CaO-SiO_2-Al_2O_3 slag system) than Fe_tO, as reported by Ohta *et al*.[17]. Over the concentration range of MnO (X_{MnO} < 0.01) in the present work, γ_{MnO} can be regarded as not being

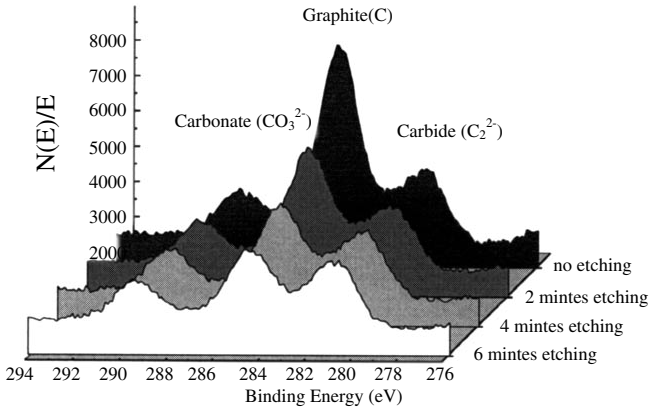

Figure 6. XPS profile of carbide, carbonate ions and graphite according to etching time

Table I
Equilibrium compositions of slag and metal at 1873 K (all figures are given as mass contents in %)

		slag								metal							
	*basicity	(CaO)	(SiO_2)	(Al_2O_3)	(MgO)	(MnO)	(Fe_tO)	(C)	(S)	(Ca)	(Si)	(Al)	(Mg)	(Mn)	(O)	(C)	(S)
1		50.30	5.4					0.05	0.173	0.001	0.024	0.001		0.448	0.000		0.000
2		0	4					30	7	2	4	9		4	7		5
3		55.20	15.					0.06	0.224	0.001	0.026	0.001		0.458	0.000		0.000
4		1	12					28	5	1	1	9		8	7		2
5		40.00	24.					0.02	0.196	0.001	0.080	0.000		0.430	0.002		0.005
6		7	26					69	6	7	1	9		9	3		4
7		42.00	4.3					0.02	0.002	0.000	0.000	0.000		0.271	0.021		0.010
8		3	4					71	1	6	0	0		4	3		4
9		41.60	4.8					0.02	0.002	0.001	0.098	0.003		0.445	0.003		0.001
1		1	3					68	3	6	5	9		2	1		2
0		36.50	3.8					0.02	0.003	0.000	0.267	0.013		0.455	0.002		0.001
1		3	1					34	4	7	6	3		0	6		1
1		41.60	7.2					0.01	0.132	0.001	0.000	0.009		0.164	0.011		0.012
1		4	8					69	3	1	3	2		7	8		7
2		40.60	8.3					0.02	0.169	0.000	0.028	0.013		0.258	0.003		0.003
1		5	2					00	1	4	2	0		7	1		6
3		40.70	8.3					0.02	0.153	0.000	0.022	0.019		0.251	0.002		0.004
1		2	9					50	0	6	2	8		1	2		0
4		42.20	8.6					0.02	0.182	0.000	0.025	0.010		0.261	0.002		0.003
1	2.76	2	5	34.06	11.15	0.17	0.24	10	2	4	6	4	0.0003	9	8	0.91	2
5	2.83	39.20	8.1	19.48	10.76	0.50	0.58	0.01	0.115	0.003	0.004	0.000	0.0004	0.167	0.007	0.91	0.017
1	1.91	2	6	19.63	17.10	0.24	0.10	67	2	0	1	8	0.0003	5	0	0.93	5
6	2.11	47.60	8.4	41.43	10.48	0.55	0.70	0.02	0.163	0.002	0.002	0.001	0.0004	0.142	0.007	0.90	0.010
1	2.02	0	4	42.36	10.48	0.04	0.05	43	4	9	5	3	0.0006	6	2	0.95	0
7	1.83	42.40	7.5	46.75	12.17	0.04	0.05	0.02	0.113	0.002	0.005	0.001	0.0005	0.144	0.008	0.87	0.013
1	2.09	5	0	39.33	12.72	0.50	1.11	01	4	9	5	1	0.0015	3	8	0.83	4
8	2.00	42.10	9.0	39.11	12.89	0.17	0.43	0.02	0.102	0.003	0.000	0.000	0.0008	0.116	0.021	0.83	0.015
1	1.98	3	5	39.55	12.89	0.19	0.35	28	1	6	0	5	0.0005	1	0	0.80	8
9	2.05	45.80	9.6	38.06	12.30	0.17	0.59	0.01	0.185	0.004	0.003	0.000	0.0006	0.251	0.004	0.85	0.003
2	2.00	1	8	39.36	13.98	0.49	1.00	67	9	5	0	4	0.0016	4	0	1.01	7
0	2.46	44.20	6.3	32.43	11.20	0.61	1.45	0.02	0.185	0.002	0.143	0.004	0.0040	0.280	0.002	0.95	0.000
2	2.18	6	8	36.98	12.36	0.61	1.03	06	7	8	9	7	0.0011	8	9	0.69	3
1	2.20	44.40	8.9	34.90	13.40	0.71	1.71	0.01	0.202	0.002	0.002	0.000	0.0009	0.268	0.002	0.91	0.001
2	2.25	2	6	34.07	12.01	0.21	0.39	36	0	3	9	9	0.0013	5	6	0.94	4
2	2.25	44.40	9.5	38.42	11.90	0.08	0.22	0.03	0.145	0.003	0.000	0.000	0.0011	0.187	0.021	0.98	0.008
2	2.18	6	3	35.77	12.08	0.11	0.13	00	1	0	0	4	0.0007	4	0	0.88	3
3	2.23	45.40	5.8	33.61	11.88	0.49	1.12	0.04	0.191	0.000	0.361	0.019	0.0008	0.298	0.002	1.07	0.003
2	2.33	6	6	38.45	11.92	0.30	0.58	72	2	8	0	2	0.0014	9	4	0.90	5
4	2.05	37.80	0.0	50.12	13.44	0.07	0.21	0.03	0.154	0.000	0.759	0.100	0.0021	0.307	0.001	0.80	0.003
2	2.18	6	9	46.68	13.31	0.07	0.22	86	8	6	0	0	0.0009	7	4	0.94	2
5	2.21	40.40	1.5	42.88	13.40	0.08	0.19	0.02	0.156	0.002	0.471	0.098	0.0006	0.292	0.001	0.95	0.002
2	2.07	9	5	38.30	13.56	0.20	0.40	70	9	1	4	7	0.0003	2	7	0.76	6
6	2.08	42.00	4.0	38.92	13.21	0.13	0.24	0.01	0.154	0.002	0.200	0.010	0.0004	0.283	0.002	1.00	0.000
2	2.12	0	8	37.80	12.76	0.13	0.46	70	9	0	8	9	0.0002	5	0	1.07	3
7	2.11	41.10	8.4	37.54	12.77	0.13	0.30	0.02	0.179	0.001	0.012	0.000	0.0002	0.262	0.013	1.15	0.002
2	1.83	6	8	14.97	18.31	0.14	0.22	43	9	7	3	9	0.0010	3	0	0.92	9
8	1.88	41.70	7.9	7.21	20.31	0.63	0.91	0.02	0.183	0.003	0.034	0.002	0.0002	0.276	0.007	1.10	0.002
2	1.84	2	6	10.48	20.66	0.40	0.87	16	7	0	5	0	0.0004	5	0	0.92	1
9	2.09	43.00	8.5	10.75	24.63	0.22	0.95	0.02	0.191	0.002	0.029	0.001	0.0004	0.265	0.006	0.98	0.001
3	1.87	8	4	23.95	16.72	0.10	0.22	31	0	2	2	1	0.0007	9	6	1.07	5
0	2.28	42.80	8.5	32.97	12.21	0.88	2.41	0.02	0.201	0.000	0.003	0.001	0.0002	0.135	0.005	0.82	0.062
3	2.19	3	9	34.89	12.31	0.67	1.29	00	3	7	3	3	0.0001	2	6	0.88	9
1	2.13	39.10	29.	34.78	12.47	1.05	3.68	0.02	0.195	0.004	0.184	0.001	0.0001	0.267	0.006	0.68	0.004
3	2.07	7	09	37.44	13.33	0.73	1.21	00	0	6	6	7	0.0005	5	4	0.81	8
2	2.16	38.80	33.	35.67	12.37	0.36	0.80	0.02	0.107	0.000	0.003	0.000	0.0001	0.171	0.003	0.96	0.030
3	2.03	5	95	38.49	13.28	0.39	0.60	89	7	8	4	8	0.0002	9	9	0.89	3
3	2.00	37.50	32.	39.34	13.88	0.54	0.67	0.03	0.139	0.001	0.017	0.000	0.0001	0.219	0.005	0.83	0.019
3	2.03	0	49	38.02	13.71	0.89	2.96	00	8	1	2	6	0.0001	0	7	0.80	6

Table I (continued)
Equilibrium composition of slag and metal at 1873K (all figures are given as mass contents in %)

4		36.7	30.					0.02	0.181	0.002	0.087	0.000		0.262	0.002		0.006
3		5	14					82	2	6	9	9		1	1		7
5		39.2	21.					0.02	0.219	0.001	0.086	0.003		0.287	0.001		0.001
3		6	76					08	6	6	4	8		8	3		2
6		44.0	9.2					0.02	0.118	0.000	0.000	0.001		0.090	0.014		0.021
3		9	8					77	0	7	0	4		6	0		5
7		43.9	9.2					0.03	0.144	0.000	0.000	0.001		0.132	0.009		0.015
3		0	4					46	7	3	0	2		1	5		8
8		40.4	8.5					0.02	0.077	0.000	0.000	0.001		0.057	0.017		0.038
3		8	4					86	3	8	3	9		5	7		7
9		40.3	8.4					0.01	0.107	0.001	0.000	0.001		0.107	0.019		0.020
		3	1					99	6	2	0	3		3	6		1
		43.6	9.1					0.02	0.175	0.000	0.000	0.001		0.205	0.004		0.006
		4	0					09	1	0	0	2		6	3		1
		40.5	8.4					0.02	0.152	0.000	0.000	0.001		0.195	0.004		0.011
		3	7					19	5	3	6	3		4	8		6
		39.1	8.1					0.02	0.126	0.001	0.000	0.001		0.155	0.004		0.016
		4	6					99	0	0	1	2		4	6		2
		38.4	8.0					0.03	0.080	0.000	0.000	0.001		0.076	0.015		0.028
		6	2					67	2	4	0	5		6	2		5

*basicity: $(X_{CaO} + X_{MgO})/(X_{SiO_2} + X_{Al_2O_3})$

Table II
Interaction parameters used in this work[10]

$i\ e_i^j\ j$ r_i^j ($r_i^{i,j}$)	Ca	Si	Al	Mg	Mn	O	C	S
Ca	-0.002 -	-0.097 0.0009	-0.072 0.0007	- -	-0.0156 -	-9000[1)] or –2500 $3.6*10^6(2.9*10^6)$ or $2.6*10^5(2.1*10^5)$	-0.34 0.012	-336 -
Si	-0.067 -	0.11 -0.0021	0.058 -	-0.1 -	0.002 -	-0.23 -	0.18 -	0.056 -
Al	-0.047 -	0.056 -0.0006	0.045 -0.001	-0.13 -	- -	-6.9 7.5(9.05)	0.091 -0.004	0.03 -
Mg	- -	-0.09 -	-0.12 -	- -	- -	-560 23000(30000)	0.15 -	-1.38 -
Mn	-0.023 -	0 0	- -	- -	0 0	-0.083 -	-0.07 -	-0.048 -
O	-3600 or -990 $5.7*10^5(2.9*10^6)$ or $4.2*10^4(2.1*10^5)$	-0.131 0	-4.06 2.67(9.05)	-370 $10^4(3*10^4)$	-0.021 0	-0.2 -	-0.45 -	-0.133 0
C	-0.097 -	0.08 0.0007	0.043 -0.0007	0.07 -	-0.012 -	-0.34 -	0.14 0.0074	0.046 -
S	-269 -	0.063 0.0017	0.035 0.0009	-1.82 -	-0.026 0	-0.27 -	0.11 0.0058	-0.028 -0.0009

1) [%Ca]+2.51[%O]<0.005 2) [%Ca]+2.51[%O]=0.005~0.016

affected by MnO content. Basicity and carbon in slag are the only affecting factors on γ_{MnO}. From the opposite tendencies of γ_{Fe_tO} and γ_{MnO} according to carbon in slag, it can be considered that the carbon has two different properties, viz. existing forms in slag. Therefore, it is necessary to investigate the stable carbon forms at a given condition (oxygen potential and slag basicity).

A wet chemical method for carbonate and carbide analyses uses a powder slag sample to facilitate the melting of the sample by acid. As previously mentioned in the experimental, an adsorbed carbon exists on the sample surface causing analytical errors. In this regard, the XPS is considered more accurate than the wet chemical method because it does not require powder samples.

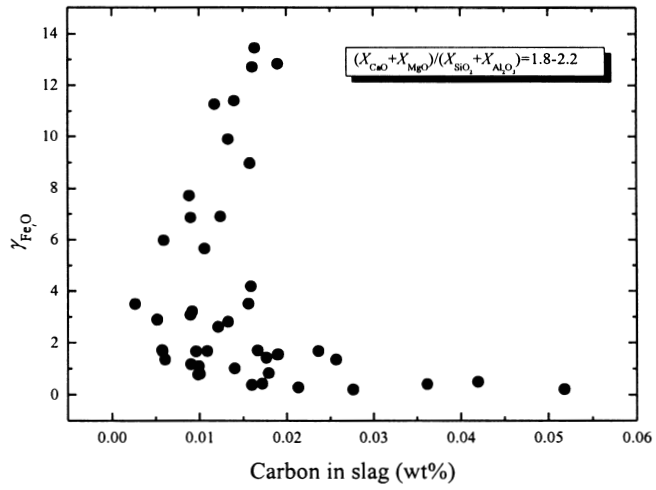

Figure 7. Effect of carbon in slag on the activity coefficient of Fe_tO

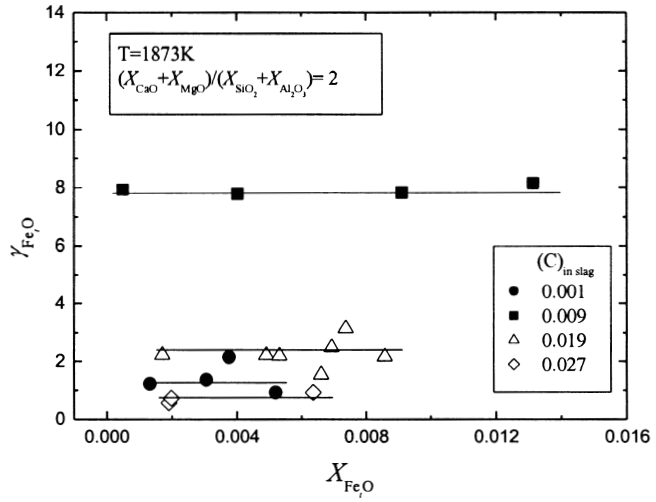

Figure 8. Activity coefficient of Fe_tO according to its mole fraction in slag (present work)

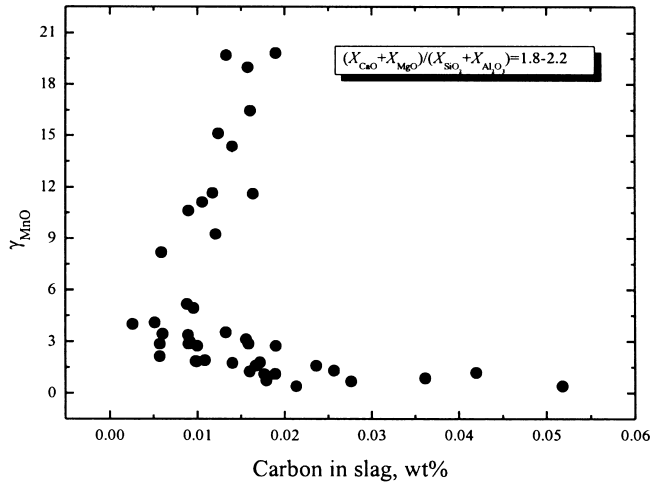

Figure 9. Effect of carbon in slag on the MnO activity coefficient

Figures 11 to 14 show the dominant carbon species in slag according to P_{O_2} at a constant basicity. P_{O_2} is determined using the following equation:

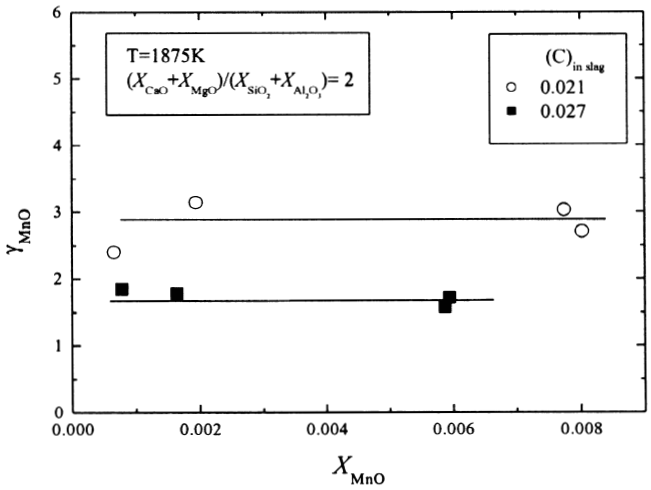

Figure 10. Activity coefficient of Fe_tO according to its mole fraction in slag (present work)

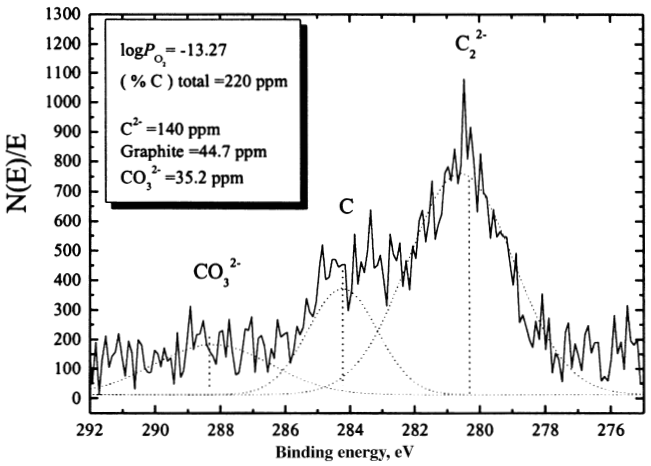

Figure 11. XPS result of carbon in slag at log P_{O2} = -13.27

$$1/2O_2 = \underline{O}$$
$$\Delta G_5^O = -117{,}000 - 2.9T \quad \text{J/mol}^{15} \qquad [5]$$

The value of can be obtained from Equation [5] by using the experimental results in Table I, as well as the respective interaction parameters in Table II.

At low P_{O_2} (=$10^{-13.27}$ atm), carbide ions are the dominant species but carbonate ions and graphite also coexist as shown in Figure 11. It means that carbide is more stable at low P_{O_2} and occupies the most of total carbon. At a little higher P_{O_2} (=$10^{-12.88}$ atm), carbide still dominates but decreased somewhat and carbonate increased relatively as shown in Figure 12. This implies that carbonate becomes the more stable species by increasing oxygen partial pressure. In Figure 13, the carbide does not exist in slag any more and only carbonate and graphite consist of the total carbon. Finally, at the highest P_{O_2} (=$10^{-9.9}$ atm), only carbonate increases in Figure 14. Consequently, it is suggested that the stable form of carbon converts from carbide to carbonate with increasing oxygen partial pressure.

From the XPS results, it can be concluded that carbide form is stable on reducing and carbonate on oxidizing atmosphere. These phenomena can be explained

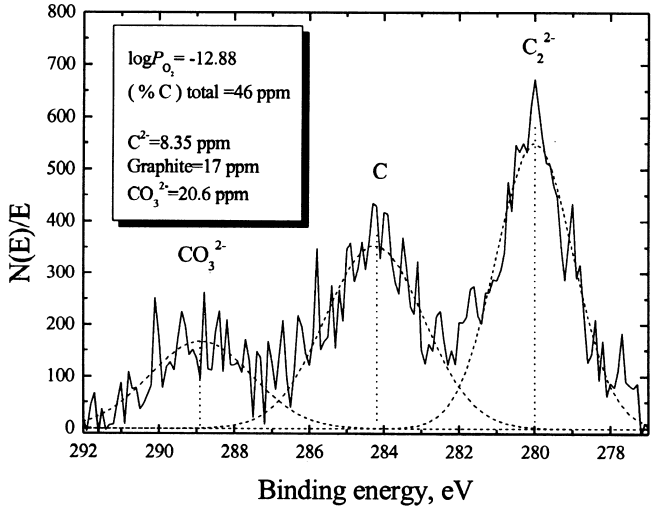

Figure 12. XPS result of carbon in slag at log P_{O2} = -12.88

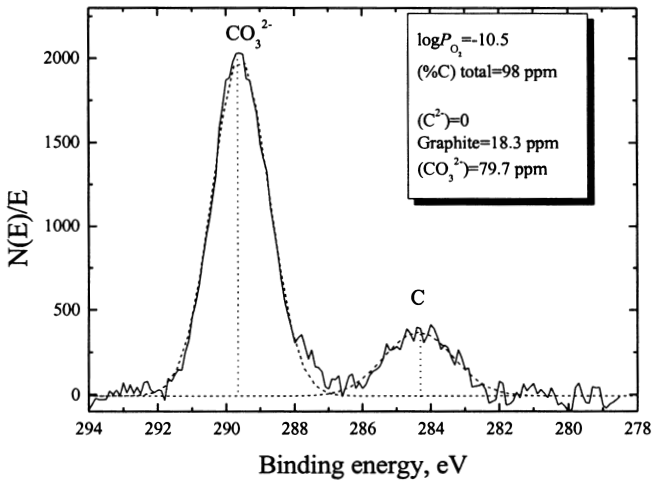

Figure 13. XPS result of carbon in slag at log P_{O2} = -10.5

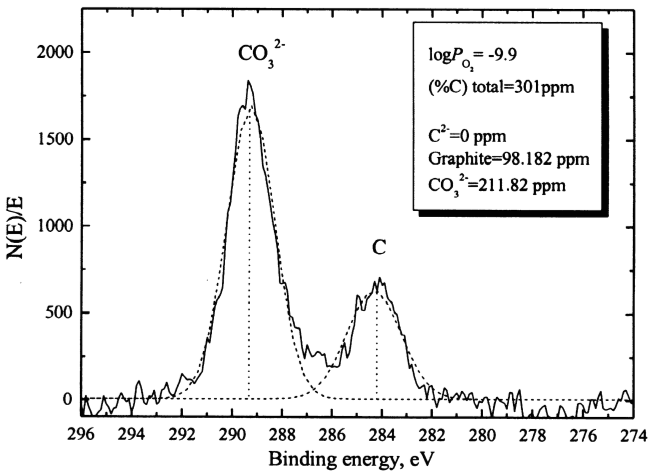

Figure 14. XPS result of carbon in slag at log P_{O2} = -9.9

thermodynamically as follows. At $P_{O_2} < 10^{-12}$, carbon is known to dissolve into slags by the following reaction[9,19–21]:

$$2\underline{C} + \left(O^{2-}\right) = \left(C_2^{2-}\right) + \frac{1}{2}O_2 \qquad [6]$$

$$K_6 = \frac{a_{C_2^{2-}} P_{O_2}^{1/2}}{a_C^2 a_{O^{2-}}} \qquad [7]$$

where K_6, a_i, and P_{O_2} are the equilibrium constant of Equation [6], the activity of i, and oxygen partial pressure, respectively. Because the carbon in metal was fixed, the following relation could be deduced:

$$\log\left(\text{mass}\%C_2^{2-}\right) = -1/2\log P_{O_2} + \log a_{O^{2-}} - \log f_{C_2^{2-}} + \log K_6 \qquad [8]$$

where $f_{C_2^{2-}}$ is the activity coefficient of C_2^{2-} ions. From Equation [8], carbon in slag is expected to increase with decreasing oxygen partial pressure with a form of carbide under a fixed composition and temperature.

Whereas, at $P_{O_2} > 10^{-10}$, it is well known that carbon is dissolved as carbonate ions, and CO_3^{2-} into molten slag[3]. Therefore, the following hypothetical slag-metal reaction can be considered:

$$\underline{C} + \left(O^{2-}\right) + O_2 = \left(CO_3^{2-}\right) \qquad [9]$$

$$K_9 = \frac{a_{CO_3}^{2-}}{a_C a_{O^{2-}} P_{O_2}} \qquad [10]$$

The following relation is obtained by using the equilibrium constant of reaction (10), K_{10}:

$$\log\left(\text{mass}\%CO_3^{2-}\right) = \log P_{O_2} + \log a_{O^{2-}} \log f_{CO_3^{2-}} + \log K_{10} \qquad [11]$$

where $f_{CO_3^{2-}}$ is the activity coefficient of CO_3^{2-} ions. From Equation [11], carbon in slag increases by increasing oxygen potential with a form of carbonate.

The XPS results prove that there are stable carbon forms in slag such as carbonate, carbide ions and graphite. This paper attempts to explain the different tendencies of γ_{Fe_tO} and γ_{MnO} using the stable carbon forms. The plots of γ_{Fe_tO} and γ_{MnO} with the oxygen potential in metal are shown together with those with carbon in slag as shown in Figures 15 and 16, respectively.

The data in Figure 15 and Figure 16 are classified in to three groups I, II, and III. From the right plots in Figure 15 and Figure 16, it is known that groups I and III (high and low P_{O_2}) are carbonate and carbide dominant regions, respectively, and those ions coexist in the group II region (intermediate P_{O_2}). In the group I region, γ_{Fe_tO} and γ_{MnO} increase with increasing carbon, viz. increasing carbonate ion in slag. For group III, they decrease with increasing carbon, viz. increasing carbide ion in slag. Therefore, it can be concluded that carbonate plays a role in increasing γ_{Fe_tO} and γ_{MnO}, and that carbide takes part in decreasing them. The carbon in steelmaking slag increases its reoxidation degree with a form of carbonate and decreases it with a form of carbide. From the viewpoint of minimizing the thermodynamic potential of reducible oxides for steel reoxidation, the carbon content in a secondary refining slag should increase with a form of carbide under conditions of reducing atmosphere.

The present results can be applied to the actual ladle refining process in order to facilitate steel cleanliness maintaining high (Fe_tO + MnO) content in steelmaking slags. The bare surface of the molten metal is formed through the slag layer by bottom gas bubbling shown in Figure 17. If carbon powder is injected on the slag/metal interface and dissolved into the effective interfacial region, the carbon content will be locally equilibrated and temporarily increased at the interfacial region. Provided

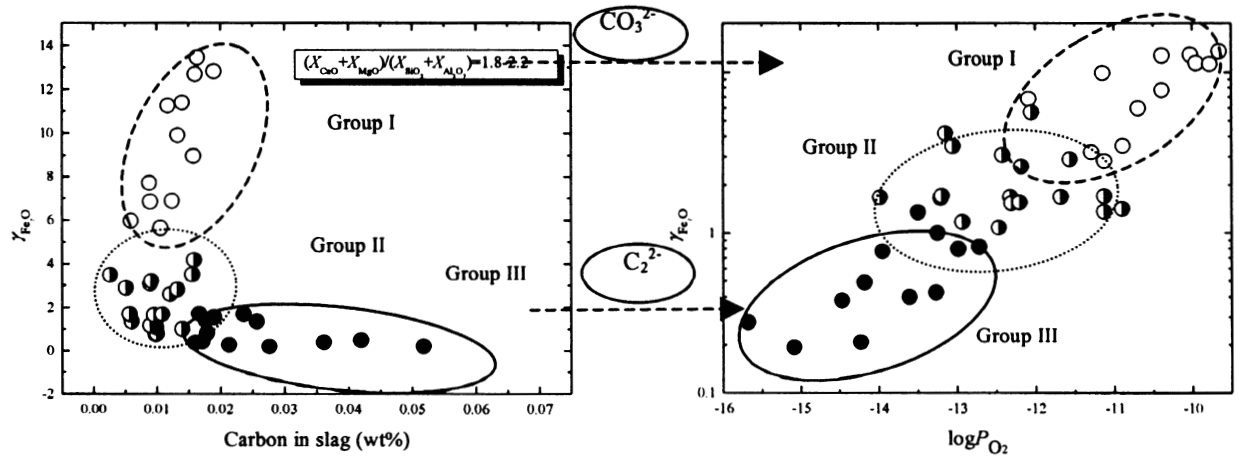

Figure 15. Relationship of carbon forms in slag and activity coefficient of Fe_tO

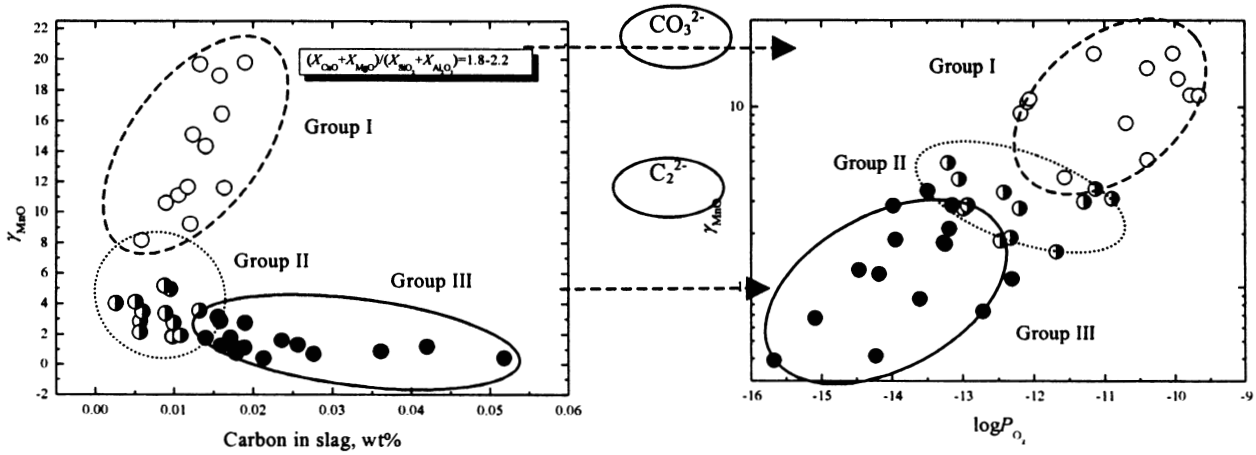

Figure 16. Relationship of carbon forms in slag and MnO activity coefficient

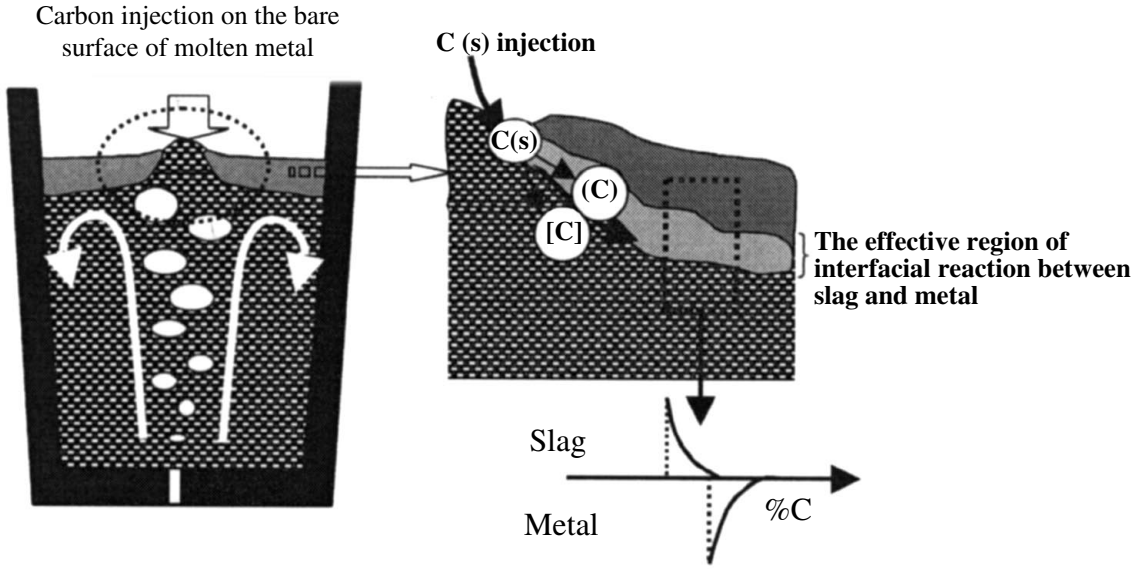

Figure 17. Schematic diagram of carbon input into the slag/metal interface

that the reducing atmosphere, γ_{Fe_tO} and γ_{MnO} are depressed at the metal/slag interface, as discussed in Figure 15 and Figure 16, as a result of the increment of carbide in slag. Consequently, the thermodynamic potential for the steel reoxidation forming the Al_2O_3 inclusion is diminished at the slag/metal interface at which real reoxidation reactions happen and therefore, the steel cleanliness is improved even though (Fe_tO + MnO) content is kept relatively high.

Conclusions

An equilibrium study of ladle refining slag systems containing carbon in slag (<600 ppm) was performed to investigate the activity coefficient of Fe_tO and MnO in terms of steel reoxidation by reducible oxides, as well as XPS analyses relating to the stable carbon forms in slag according to oxygen partial pressure.

The activity coefficients of Fe_tO and MnO show identical diverging trends, with increasing carbon content showing increment and decrement at the same time. XPS results prove that carbon dissolves in steelmaking slag as carbonate and carbide forms under oxidizing and reducing atmospheres, respectively. A simultaneous consideration of Fe_tO and MnO and stable carbon forms in slag was needed to thermodynamically explain the trend of γ_{Fe_tO} and γ_{MnO} according to carbon content. From the above relation, it was found that carbonate played a role in increasing γ_{Fe_tO}, and γ_{MnO} and carbide took part in decreasing them. In other words, the dissolved carbon in a steelmaking slag increases the reoxidation degree with a form of carbonate and decreases it with a form of carbide.

Finally, this paper suggested that the thermodynamic potential for the steel reoxidation by reducible components could be repressed by increasing the carbon in slag with a form of carbide at the metal/slag interface by injecting carbon powder at the bare surface of molten metal in real plant work.

References

1. JO, S.K. and KIM, S.H. Thermodynamic assessment of CaO-SiO_2-Al_2O_3-MgO-Cr_2O_3-MnO-Fe_tO slags for refining chromium-containing steels. *Steel Research*, vol. 71, no. 8, 2000, pp. 281–287.
2. LEE, K.R. and SUITO, H. Solubilities of carbon in CaO-Al_2O_3-SiO_2 slags saturated with liquid iron. *Process Metallurgy*, 1995, pp. 98–103.
3. KUWATA, M. and SUITO, H. Solubility of carbon in CaO-Al_2O_3 melts. *Metallurgical and Materials Transactions B*, vol. 27B, 1996, pp. 57–64.
4. SWISHER, J.H. Thermodynamics of carbide formation and graphite solubility in the CaO-$SiO_2Al_2O_3$ system. *Transactions of the Metallurgical Society of AIME*, vol. 242, 1968, pp. 2033–2037.
5. PARK, J.H. and MIN, D.J. Thermodynamic behavior of carbon in molten slags. *ISIJ International*, vol. 40, supplement, 2000, pp. S96–S100.
6. MORI, M., MORITA, K, and SANO, N. Dependence of carbon solubility on oxygen partial pressure for 80 mass pct BaO-MnO and CaO_{satd}-B_2O_3 slags. *Metallurgical and Materials Transactions B*, vol. 28B, 1997, pp. 1257–1259.
7. PARK, E., ZHANG, J., THOMSON, S., OSTROVSKI, O. and HOWE, R. Characterization of phases formed in the iron carbide process by X-ray diffraction, Mossbauer, X-ray photoelectron spectroscopy, and Raman spectroscopy analyses. *Metallurgical and Materials Transactions B*, vol. 32B, 2001, pp. 839–845.
8. SEO, J.D. and KIM, S.H. Thermodynamic assessment of Mg deoxidation reaction of liquid iron and equilibria of [Mg]-[Al]-[O] and [Mg]-[S]-[O]. *Steel Research*, vol. 71, no. 4, 2000, pp. 101–106.
9. SONG, H.S. Thermodynamic behaviors of carbon and nitrogen dissolution in steelmaking slags. Doctoral Thesis in POSTECH, 1997, pp. 100–101.
10. BERRYMAN, R.A. and SOMMERVILLE, I.D. Carbon solubility as carbide in calcium silicate melts. *Metallurgical Transactions B*, vol. 23B, 1992, pp. 223–227.
11. CHRISTIE, AB., SUTHERLAND, I., and WALLS, J.MSS. X.P.S. study of the angular dependence of preferential sputtering and ion-induced reduction in lead oxide-containing glasses. *Vaccum.* vol. 34, 1984, pp. 659–662.
12. PALCHAN, I., CRESPIN, M., ESTRADE-SZWARCKOPF, H., and ROUSSEAU, B. Graphite Fluorides—an XPS study of a new type of C-F bonding. *Chemical Physics Letters*, vol. 157, Iss 4, 1989, pp. 321–327.
13. PAPARAZZO, E., DORMANN, J.L., and FIORANI, D. X-Ray Photoemission Spectroscopy (XPS) Analysis of $Fe_{82}B_{18}$-Al_2O_3 Granular Systems. *Solid State Commun.*, vol. 50, no. 10, 1984, pp. 919–823.
14. SUITO, H. and INOUE, R. Thermodynamic Considerations on Manganese Equilibria Between Liquid Iron and Fe_tO-MnO-MO_x (MO_x = $PO_{2.5}$, SiO_2, $AlO_{1.5}$, MgO, CaO) Slags. *Trans. Iron Steel Inst. Jpn.*, vol. 24, no. 4, 1984, pp. 301–307.
15. SIGWORTH, G.K. and ELLIOTT, J.F. Thermodynamics of Liquid Dilute Fe Alloys. *Met. Sci.*, vol. 8, no. 9, 1974, pp. 298–310.
16. SEO, J.D., KIM, S.H., and LEE, K.R. Thermodynamic assessment of the Al deoxidation reaction in liquid iron. *Steel Research*, vol. 69, 1998, pp. 49–53.
17. OHTA, H. and SUITO, H. Activities of MnO in CaO-SiO_2-Al_2O_3-MnO(Less-Than-10 Pct)-Fe_tO(Less-Than-3 Pct) Slags Saturated with Liquid-Iron. *Metallurgical and Materials Transactions B*, vol. 26B, 1995, pp. 295–303.
18. GAYE, H., GATELLIER, C., and NADIF, M. Slags and Inclusions Control in Secondary Steelmaking. *Rev. Metall., Cah. Inf. Tech.*, vol. 84, no. 11, 1987, pp. 759–771.
19. SONG, H.S., RHEE, C.H., and MIN, D.J. Thermodynamic Behavior of Carbon in CaO-SiO_2 Slag System. *Steel Research*, vol. 70, 1999, pp. 105–109.
20. PARK, J.H. and MIN, D.J. Solubility of Carbon in CaO-B_2O_3 and BaO-B_2O_3 Slags. *Metallurgical and Materials Transactions B*, vol. 30B, 1999, pp. 1045–1052.
21. SOHN, I., MIN, D.J., and PARK, J.H. Thermodynamic Study on the Effect of CaF_2 on the Nitrogen and Carbon Solubility in the CaO-Al_2O_3-CaF_2 Slag System. *Steel Research*, vol. 70, 1999, pp. 215–220.